Hands-On Experience with UWB: Angle of Arrival Accuracy Evaluation in Channel 9

Radovan Juran[1], Petr Mlynek[1], Martin Stusek[1], Pavel Masek[1], Michal Mikulasek[1], and Aleksandr Ometov[2]

[1]Department of Telecommunications, Brno University of Technology, Brno, Czech Republic
[2]Unit of Electrical Engineering, Tampere University, Finland
✉Contact author's e-mail: masekpavel@vut.cz

***Abstract*—This paper evaluates IEEE 802.15.4z standard-compliant NXP SR040 and SR150 chips in Angle of Arrival (AoA) capabilities in Channel 9 (7.737—8.237 GHz) of the Ultra-WideBand (UWB) spectrum. Due to the shorter wavelength, higher frequencies may encounter certain limitations when it comes to harsh environments, as more reflections and multipath propagation can occur. Furthermore, they also can be affected by their enclosure used to protect the electronics in such an environment, which needs to be taken into account during product design. This work presents the results of the evaluation measurement scenario relatable to real-life use cases and concludes potentially valuable insight important for consideration when creating a new UWB product. Besides a basic overview of the theoretical estimation of AoA by Time Difference of Arrival (TDoA) and Phase Difference of Arrival (PDoA), and the evaluation of the corresponding results, the main contribution is the repeatable topology considered for the conducted measurements. The presented results allow vendors to compare their solutions with the various radio chips or antenna configurations.**

***Index Terms*—Angle of arrival (AoA), line of sight (LoS), Ultra wideband technology (UWB)**

I. Introduction

Although Ultra-Wideband (UWB) has been known for several decades, it is experiencing a renaissance and gaining momentum in recent years, mainly due to the expansion into more fields – mobile phones, wearables, automotive or industrial applications. This significantly stimulates innovation and integration of UWB radio chip solutions and other related radio (RF) components (antennas and parts of the whole radio front-end part). As a result, the estimated number of sold UWB chips is expected to further grow at least by 2025, as presented in [1], [2], which in terms of numbers means over 1 billion annual UWB technology-enabled device shipments, especially in consumer electronics like mobile phones, which will open new opportunities along with new challenges to cope with [3].

One of these challenges might be adoption of higher UWB channels, such as Channel 9 discussed in this work. The main reason is that with growing frequency, the wavelength shortens and thus influences the needs of the RF front-end, including the antennas and enclosure designs, as the wavelength might be close to the dimensions of used enclosures (material and its thickness, screws, etc.). Therefore it is valuable to evaluate the performance of available hardware, discuss the results, and set the ground for further complex testing and detailed evaluation measurements.

This paper is further structured into sections as follows: (ii) Theoretical principles, where the mathematical background of measured quantities is presented; (iii) Related works regarding evaluated integrated circuits; (iv) Method of Measuring, where the used hardware and tools are briefly presented along with description of the measurement scenario and environment assessed; (v) Achieved Results and Discussion, and finally the (vi) Conclusion section with statements based on the results and observations from the conducted experiments.

II. Theoretical Principles

A brief explanation of principles used for estimation of the ranging parameters is presented in this section. The principles of the Phase Difference of Arrival (PDoA) and Angle of Arrival (AoA) estimation are based on trigonometric functions from corresponding triangles and relationships of distance, time, and velocity [4]. To illustrate these relationships, Fig. 1 below shows the derivation of equations for PDoA estimation in a two-antenna array.

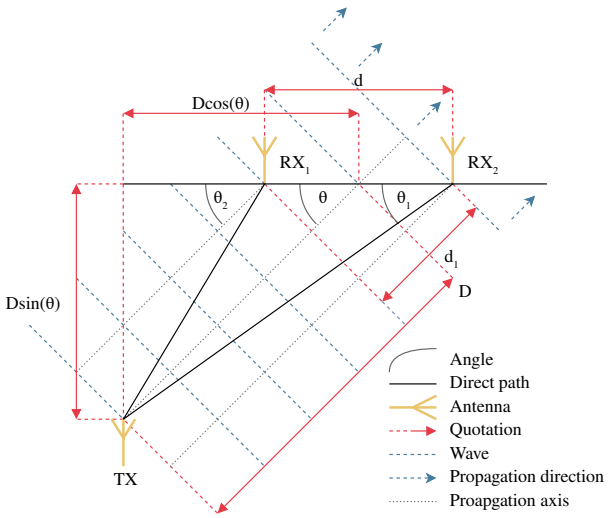

Fig. 1: Geometry for Phase Difference of Arrival (PDoA) estimation.

The two receiving antennas RX_1, RX_2 are at a distance d from each other. The distance between the axis of the receiver antenna array and the transmitter antenna TX is denoted by D.

The angle subtended from the plane of the antenna array to the direct path is denoted by θ, or θ_1 for *TX-RX1* and θ_2 for *TX-RX2*, nonetheless for distances greater than a few wavelengths λ, when $D \ll d$, it is possible to use $\theta_1 = \theta_2 = \theta$. Then, trigonometric functions and the similarity of triangles can be applied to derive the relationships below.

As soon as the wave-front of the propagating wave reaches the first receiving antenna, the wave with the speed of light c still has to travel to the second antenna over the distance $d_1 = dsin(\theta)$, which, since velocity is distance over time, will happen in time

$$t_1 = \frac{dsin(\theta)}{c}, \tag{1}$$

also known as the Time Difference of Arrival (TDoA), depicted illustratively in Fig. 2.

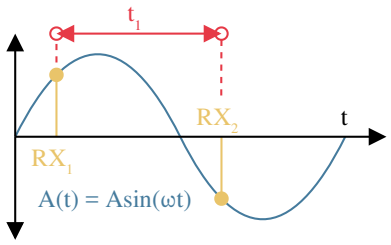

Fig. 2: Phase Difference of Arrival (PDoA) estimation.

To conclude the theory explanation and derive an equation for PDoA and AoA estimation, a simple carrier wave is depiceted in Fig. 2. It can be described as

$$A(t) = Asin(\omega t) = Asin(\varphi), \tag{2}$$

where φ is the phase of the wave received on RX_1 as φ_1 and RX_2 as φ_2, delayed by t_1. Now, the difference is derived as

$$\Delta\varphi = \varphi_2 - \varphi_1 = 2\pi f(t + t_1) - 2\pi f = 2\pi f t_1. \tag{3}$$

Further, by using t_1 derived in (1) and knowing that 2π in radians represents 360° and wavelength is defined as

$$\lambda = \frac{c}{f}, \tag{4}$$

it is possible to write the following relation for PDoA

$$\Delta\varphi = \frac{360°}{\lambda} d \cdot sin(\theta), \tag{5}$$

from which the AoA can be expressed as follows:

$$\theta = sin^{-1}\left(\frac{\Delta\varphi}{360°}\frac{\lambda}{d}\right). \tag{6}$$

This is considered for antennas of nearly ideally identical radiation patterns with negligible effects of mutual coupling. To achieve correct $\Delta\varphi$ to θ mapping, for distance d between antennas there is a condition $d < \frac{\lambda}{2}$ for interval $\theta = [\frac{-\pi}{2}, \frac{\pi}{2}]$ angle [4].

III. Related Work

Regarding hands-on experiments with AoA estimation using real-world hardware, there are only several similar studies assessing measured values of AoA utilizing UWB radio and PDoA. Still, all of them rely on different types of UWB integrated circuits, none of them being produced by NXP.

The authors of [4] present results achieved with Qorvo Decawave DW1000 chips in a small anechoic chamber, in other words, in an ideal environment. The same chips were used by [5], where authors also present results achieved with DW1000 chips bringing performances analysis of an AoA using PDoA kit, reaching maximal error of 10° in an ideal environment with planar antennas. Both studies show that overall errors in AoA estimation are produced by the electromagnetic effects in the anchor (receiver) antenna array rather than on-chip PDoA measurement inaccuracy when an ideal environment is considered.

TABLE I: Published works mentioning SR040 and SR150.

No.	Year	Context mentioning the NXP chips
[6]	2022	This research work provides a comparison of several commercially available UWB localization modules. Modules are compared instead based on technical specifications than real-world measurements.
[7]	2022	The main goal of this work is to evaluate the possibility of cross-technology interferences between UWB and WI-Fi 6E. For this purpose, Decawave DW1000 and Qorvo DW3000 in different physical layer settings were used.
[8]	2022	This paper compares UWB and Bluetooth localization accuracy in an office environment for both LoS and NLoS scenarios. Notably, the work relies on the utilization of DW1000 since NXP SR040 was not available at the time of the research.
[9]	2022	Research thoroughly compares currently available UWB radio chips in terms of compatibility and basic functionality. The main focus is given on interoperability and compatibility issues related to physical, medium-access-control, and upper layers.
[10]	2021	This paper evaluates a practical over-the-air attack on IEEE 802.15.4z high-rate pulse repetition frequency (HRP) UWB distance measurements systems. Notably, the attack is conducted on several off-the-shelf UWB chips, including NXP SR040 and SR150.
[11]	2021	Research work focused on the security analysis of UWB HRP mode. Notably, multiple attacks and countermeasures for HRP mode are discussed.
[12]	2021	Recently published doctoral thesis dealing with UWB security. The work introduces the UWB pulse recording modulation scheme and enlargement attack detection for security improvements of the UWB standard.
[13]	2021	Bachelor thesis focused on the design of a UWB board prototype for localization. On top of that, currently available UWB chips are discussed, and a comparison is made. Finally, an initial analysis of location accuracy is given.

Meanwhile, in [14], a testbed with Arbitrary Waveform Generator (AWG), oscilloscope, and a computer running Matlab is used to evaluate the influence of UWB antennas on the AoA estimation, also stating the conclusion that the

performance of AoA estimation is considerably influenced mainly by the receiving antennas on the anchor receiving antenna array.

Yet still, both transmitter and receiver antennas were always of different types and configurations, as well as methods of data acquisition and calculation or different UWB channels were used in these types of studies. This makes their results rather incomparable against each other. On top of that, to our best knowledge, none of the available publications evaluates AoA estimation capabilities in the new UWB Channel 9. Therefore, examples are selected to utilize the measurement approach, as a comparison of the results would be out of the context of this report and require a more extensive, dedicated research and overview. However, sources mentioning measurements and evaluation based explicitly on the *NXP Trimension SR040 and SR150* (see section IV) are not that plentiful, as Tab. I suggests, many of them often contain only informative mention of them and do not provide any practical evaluation.

Consequently, results of any experiment with the newest NXP hardware can be considered a potential contribution when it comes to their practical evaluation in a real-world scenario.

IV. Measurement Environment and Scenario

The NXP revealed the Trimension SR040 and SR150 integrated circuits implementing the IEEE 802.15.4z standard [15], which currently is in Revision 802.15.4-2020 [16]. These chips were made accessible for evaluation by Mobile Knowledge as an evaluation set of tags and anchor called MK UWB Kit [15], used for the measurements in this paper. The radio part of the anchor equipped with SR150 is based on Amotech module ASMOP1BO0N1 [17], which is complemented by two external surface-mount devices (SMD) antennas by the same manufacturer. At the same time, the RF circuitry of the tag builds directly upon the SR040 and a planar antenna on the tag's printed circuit board (PCB). Furthermore, both tag and anchor utilize the NXP QN9090 MCU with Bluetooth Low Energy 5.0, and near field communication (NFC) [18].

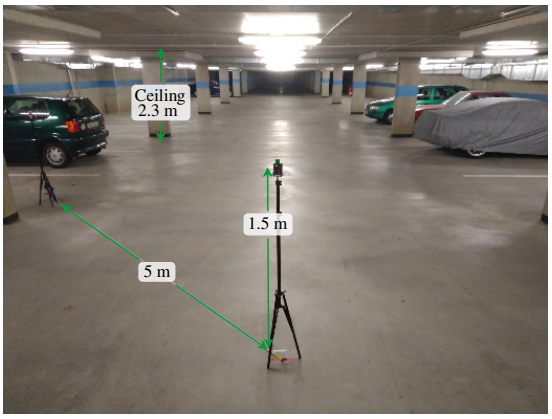

Fig. 3: Photo of the measurement setup in the underground parking lot.

For experimental testing and measurement evaluation, selecting an adequate environment that should match the conditions and parameters of the potential deployment in real scenarios is crucial. For this report, an indoor underground parking lot was chosen, depicted in Fig. 3 below, as it resembles a typical industrial-like UWB indoor scenario.

Both the tag and the anchor were located approximately 1.5 m above ground using tripods and under direct line-of-sight (LoS) conditions. For precise angle adjustment, a commercial device Edelkrone HeadOne [19] was used. Consequently, angles were set in the interval from -45° to +45° with the step of 15° and the angle of 0° being in the center of direct LoS. This measurement was performed in three separate phases, changing the distance between tag and anchor from 5 m to 20 m and 30 m, always in a static position.

V. Results and Discussion

The obtained data can be viewed in many different contexts and mutual relationships, with the most interesting ones presented in this section.

In the first set of measurements, the PDoA accuracy in relation to the angle of incidence was evaluated as it represents the base of AoA estimation. The red dashed line depicted in Fig. 4 is a value based on a formula (2) representing phase shift in an optimal condition without distortion from interferences in the signal path. According to expectations, the deviation is the lowest when the angle is zero and rises with the growing angle. Surprisingly, the inaccuracy of PDoA estimation for the negative half-plane is the highest for the angle of -30° but decreases significantly at -45°. This behavior can be caused by the uneven antenna radiation pattern or caused by the reflected wave causing interferences with the main beam. For the positive half of the diagram, this behavior can be seen only for a 20 m distance. However, for 45°, the inaccuracy rises for all TX and RX separation distances. Finally, it can be seen that the PDoA estimation accuracy decreases with the rising distance. It is not critical for small angles (-15° to 15°), but it is more pronounced for larger angles.

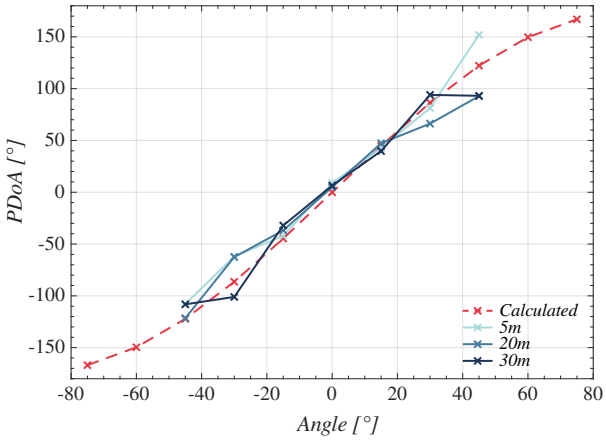

Fig. 4: Measured PDoA.

Further, as the PDoA plays a crucial role in AoA estimation, it can be assumed that the influence of PDoA will also be

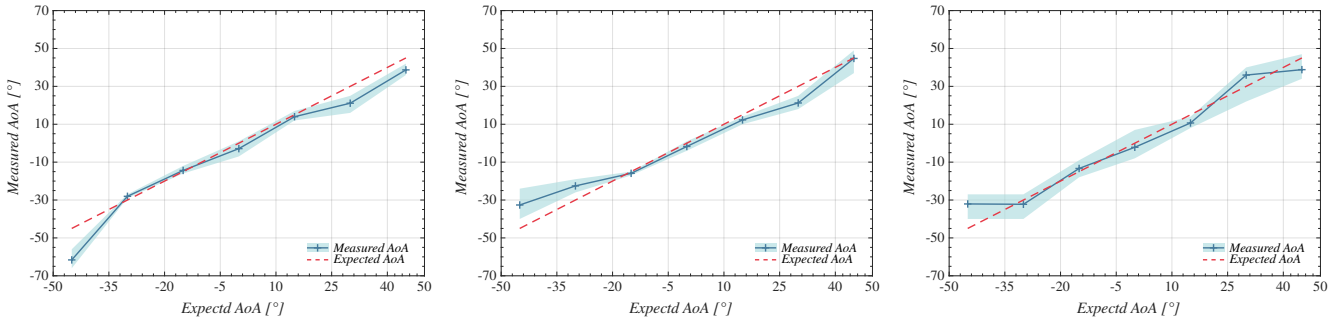

(a) 5 m distance. (b) 20 m distance. (c) 30 m distance.

Fig. 5: AoA measured at varying distance.

observable on the accuracy of AoA results. As seen in Fig. 5, the practical measurements verify this assumption. Notably, the red dashed line represents the expected value of AoA, whereas the filled blue area shows boundaries of maximal and minimal mastered AoA values, with the solid line standing for the mean value.

The measurement results further verify the initial idea of declining AoA estimation accuracy with the rising distance between receiver and transmitter. This is evident especially for the maximum and minimum estimation boundaries, which significantly expand with the increasing distance of devices (most pronounced for 30 m separation). Notably, the accuracy of AoA estimation is surprisingly higher for 20 m distance compared to 5 m separation. It can be caused by a smaller contribution of reflected waves on the resulting signal waveform. In the case of a 5 m distance, the reflected beams may represent a significant part of the total amplitude. However, for a 20 m distance, the influence of these rays is negligible. Nevertheless, in the case of averaged values, these inaccuracies are significantly reduced, which means that it is possible to increase the AoA estimation accuracy by averaging values from multiple measurements.

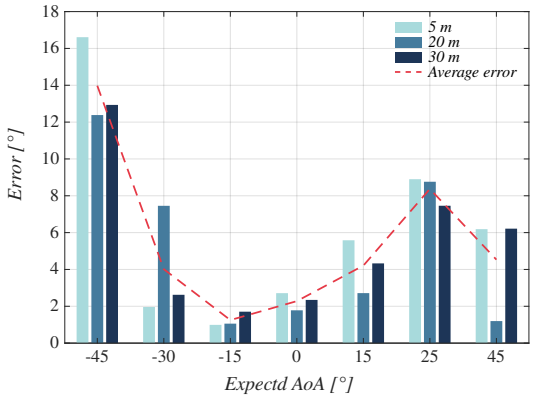

Fig. 6: Errors in angle estimation.

Finally, Fig. 6 summarizes errors of AoA measurement in absolute values on the vertical axis for each set (expected) angle on the horizontal axis. The trend of average error distribution being larger in the left half-plane compared to the right half-plane, which is in line with other similar works [4]. It is also further verified that the AoA estimation accuracy is higher for 20 m distance compared to both 5 m and 30 m, but only for smaller angles (-15° to 15°).

Notably, all the tests presented in this paper to this part were performed with bare electronics without considering any enclosure, vital for any practical industrial use-case. However, especially in UWB Channel 9, which means around the center frequency of 8 GHz, it is potentially probable that when put in an enclosure of a not adapted design, the frequency might be high enough to alter the radiation pattern of the tag, as using (4) the $\lambda/2 = 0.018$ m, which is in order of dimensions of common universal enclosures [20]. Therefore for the closest range of 5 m distance, the measurement was repeated with the tag being enclosed in a standard universal box [20] to assess the possible influence of an enclosure. Although the results in Fig. 7 copy the trend in behaviour observable in plots in Fig. 5, there is a slight observable discrepancy when the tag is enclosed.

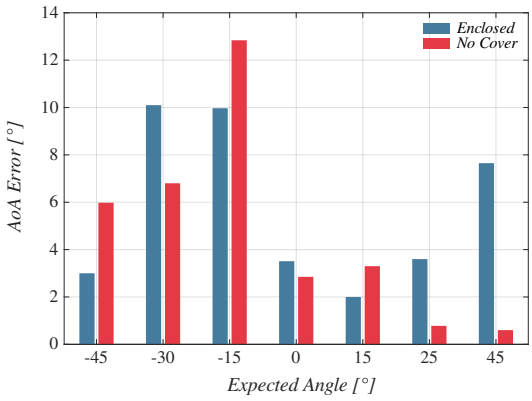

Fig. 7: AoA estimation error in relation to use of an enclosure.

VI. Conclusion

This paper presents evaluation results of the new UWB chips by NXP, namely the SR150 and SR040, in terms of AoA capabilities in UWB Channel 9 using space-efficient SMD receiving antennas.

Although there were some significant errors reaching over 10° in some of the AoA estimations, it has to be emphasized that these were achieved only with a receiver's build-in pair of SMD antennas. From the results it can be seen that with distance the accuracy of AoA estimation drops, which is consistent with the assumption that the accuracy is significantly affected by the antenna array electromagnetic parameters rather than the capabilities of the radio chip itself. Therefore with a better antenna array, an improvement in AoA estimation accuracy can be expected even for greater distances between the tag and the anchor. Also, from the results of measurement with and without an enclosure, it seems that the design of the used enclosure has the capability to influence the estimation at higher frequencies of UWB Channel 9, as it influences the tag antenna.

Future work could introduce more sample granularity, as it would give a better overall image, even if there are significant errors near the edges of the evaluated interval, as this work brings results measured only in an interval of $<-45^\circ, +45^\circ>$. Also, even if the experiments were conducted in a real environment, only clear line-of-sight path was considered, so evaluation of various LoS and nLoS scenarios would also broaden the image.

Acknowledgment

For the research, the infrastructure of the SIX Center was used. This work was supported by the Technology Agency of Czech Republic project No. FW03010424.

References

[1] Techno Systems Research (TSR), "2020 Ultra Wideband Market Analysis," Techno Systems Research Co., Ltd., Tech. Rep., 2020. [Online]. Available: https://www.t-s-r.co.jp/en/report/3445/

[2] "Comments of The Ultra Wide Band (UWB) Alliance Before The Federal Communications Commission," 2019.

[3] A. Zignani and S. Tomsett, "Ultra-Wideband (UWB) for the IoT – A Fine Ranging Revolution?" ABIresearch, Tech. Rep., 2021. [Online]. Available: https://www.nxp.com/webapp/Download?colCode=UWBWP

[4] I. Dotlic, A. Connell, H. Ma, J. Clancy, and M. McLaughlin, "Angle of arrival estimation using decawave DW1000 integrated circuits," in *2017 14th Workshop on Positioning, Navigation and Communications (WPNC)*. IEEE, 2017, pp. 1–6. [Online]. Available: http://ieeexplore.ieee.org/document/8250079/

[5] S. Diagne, T. Val, A. K. Farota, B. Diop, and O. Assogba, "Performances Analysis of a System of Localization by Angle of Arrival UWB Radio," *International Journal of Communications, Network and System Sciences*, vol. 13, no. 02, pp. 15–27, 2020. [Online]. Available: https://www.scirp.org/journal/doi.aspx?doi=10.4236/ijcns.2020.132002

[6] R. I. Vitanov and D. N. Nikolov, "A State-of-the-Art Review of Ultra-Wideband Localization," in *2022 57th International Scientific Conference on Information, Communication and Energy Systems and Technologies (ICEST)*, 2022, pp. 1–4.

[7] M. Schuh, H. Brunner, M. Stocker, M. Schuß, C. A. Boano, and K. Römer, "First Steps in Benchmarking the Performance of Heterogeneous Ultra-Wideband Platforms," in *2022 Workshop on Benchmarking Cyber-Physical Systems and Internet of Things (CPS-IoTBench)*, 2022, pp. 34–39.

[8] M. Bilge, "Evaluation of Ultra Wide Band Technology as an Enhancement for BLE Based Location Estimation," *ArXiv*, p. 10, 2022. [Online]. Available: https://doi.org/10.48550/arXiv.2202.00558

[9] D. Coppens, E. D. Poorter, A. Shahid, S. Lemey, and C. Marshall, "An Overview of Ultra-WideBand (UWB) Standards(IEEE 802.15.4, FiRa, Apple): Interoperability Aspects and Future Research Directions," *IEEEAccess*, p. 20, 2022. [Online]. Available: https://arxiv.org/abs/2202.02190

[10] P. Leu, G. Camurati, A. Heinrich, M. Roeschlin, C. Anliker, M. Hollick, S. Capkun, and J. Classen, "Ghost Peak: Practical Distance Reduction Attacks Against HRP UWB Ranging," *ArXiv*, p. 15, 2021. [Online]. Available: https://arxiv.org/abs/2111.05313

[11] M. Singh, M. Roeschlin, E. Zalzala, P. Leu, and S. Čapkun, "Security Analysis of IEEE 802.15.4z/HRP UWB Time-of-flight Distance Measurement," in *Proceedings of the 14th ACM Conference on Security and Privacy in Wireless and Mobile Networks*. New York, NY, USA: ACM, 2021, pp. 227–237. [Online]. Available: https://dl.acm.org/doi/10.1145/3448300.3467831

[12] S. Mridula, "Securing Distance Measurement against Physical Layer Attacks," Doctoral Thesis, ETH Zürich, Zürich, 2021. [Online]. Available: https://doi.org/10.3929/ethz-b-000514834

[13] R. Ranieri, "Localizzazione indoor basata su tecnologia UWB," Thesis (Bachelor), Scuola Universitaria Professionale della Svizzera Italiana, 2021. [Online]. Available: http://tesi.supsi.ch/id/eprint/4041

[14] W. Gerok, M. El-Hadidy, S. A. El Din, and T. Kaiser, "Influence of the real UWB antennas on the AoA estimation based on the TDoA localization technique," in *IEEE Middle East Conference on Antennas and Propagation (MECAP 2010)*, 2010, pp. 1–6.

[15] MobileKnowledge, "MK UWB SR150/SR040: UWB Development Kit for Trimension™ SR150/SR040." [Online]. Available: https://bit.ly/3pBnqhh

[16] J. Goldberg, "IEEE Standard for Low-Rate Wireless Networks," *IEEE Std 802.15.4-2020 (Revision of IEEE Std 802.15.4-2015)*, pp. 1–800, 2020.

[17] NXP, "Trimension™ SR150 Module Without Antennas: AS-MOP1BO0N1." [Online]. Available: https://bit.ly/3Tco0zV

[18] NPX, "QN9090/30: Bluetooth Low-Energy MCU with Arm®Cortex®-M4 CPU, Energy Efficiency, Analog and Digital Peripherals and NFC Tag Option." [Online]. Available: https://bit.ly/3aAOCJ9

[19] "Edelkrone HeadONE." [Online]. Available: https://edelkrone-eu.com/products/headone

[20] KRADEX, "Z65J PS: Enclosures Hermetically Sealed." [Online]. Available: https://www.kradex.eu/product/enclosures_hermetically_sealed/z65?lang=en